Energy Reports 6 (2020) 2056–2065

Contents lists available at ScienceDirect

Energy Reports

journal homepage: www.elsevier.com/locate/egyr

Research paper

The crucial geometric distinctions of microfractures as the indispensable transportation channels in hydrocarbon-rich shale reservoir

Yijin Zeng [a,b], Shuheng Du [c,*], Xu Zhang [a,b], Baoping Zhang [a,b], Honglei Liu [a,b]

[a] State Key Laboratory of Shale Oil and Gas Enrichment Mechanisms and Effective Development, Beijing 100101, China
[b] Sinopec Research Institute of Petroleum Engineering, Beijing, 100101, China
[c] State Key Laboratory of Nonlinear Mechanics, Institute of Mechanics, Chinese Academy of Sciences, Beijing 100190, China

ARTICLE INFO

Article history:
Received 6 May 2020
Received in revised form 26 June 2020
Accepted 9 July 2020
Available online 12 August 2020

Keywords:
Microfracture
Transportation channels
Shale
Reservoir

ABSTRACT

This study aimed to investigate the crucial geometric distinctions of microfractures as the indispensable transportation channels in hydrocarbon-rich shale so as to find the new evidence for hydrocarbon exploration and exploitation.

This study mainly shows that (1) microfracture length and width would show a good positive linear correlation, but when the length of microfracture reaches a key point, the width of microfracture would gradually deviate from the linear relationship and gradually diverges. (2) compaction or other tectonic stress can promote the formation of shale microfractures and promote the occurrence of pressure solution. (3) Similarly, before a certain key point, the poor orientation degree of microfractures often coexists with the higher convexity of microfractures, which is positively correlated. When this key point is crossed, the two begin to show a negative correlation. This may be due to the fact that the microfractures will open, close, extend or even interlace more frequently when the rock is under complex stress conditions.

It proved that when describing the heterogeneity characteristics of microfractures, we should clearly describe them from two aspects of size and geometry so as to ensure the integrity of the conclusion.

1. Introduction

In contemporary world, unconventional oil and gas has become the major type of energy and fuel (Clarke et al., 2016; Kondash et al., 2017; Middleton et al., 2017; Du et al., 2019a; Du, 2019). Shale has become one of the most important types of unconventional reservoirs (Khan et al., 2016; Kilian, 2016; Wachtmeister et al., 2017; Du et al., 2020, 2019b). Large-scale natural fracture and hydraulic fracture have become quite popular topics in the field of both geology and mechanics (Zhao, 2016, 2018; Zhu et al., 2018; Huang et al., 2019; Zhang et al., 2019). In addition to matrix pores, microfractures widely developed in shale are the core factors for shale oil and gas to be stored and percolated (Ougier-Simonin et al., 2016; Teixeira et al., 2017; Ukar et al., 2017; Du et al., 2020). To some extent, the microfractures in shale are the "double-edged sword". On the one hand, they form the new oil and gas transportation channels, which are helpful for the flow and effective production of oil and gas (Pluymakers et al., 2017; Madasu and Nguyen, 2017); on the other hand, if the scale of microfractures reach a certain degree, when the small microfractures gather, it is possible to form a large range of macroscopic fractures (Gupta et al., 2017; Panahi et al., 2019). This is the principle that a quantitative change causes a qualitative change. In this way, it may also lead to the escape of oil and natural gas, resulting in the decrease of hydrocarbon saturation and exploitation potential of the original reservoir (Lesniak et al., 2017; Chauve et al., 2019). Therefore, characteristics of microfractures are of great significance for the enrichment and exploitation of oil and gas resources, and are worth further study.

In the aspect of shale microfracture research, scholars at home and abroad have done a lot of fruitful research in the field of type division, genetic mechanism and filling characteristics and achieved important results (Abouelresh, 2017; Elwegaa and Emadi, 2019; Mohammadmoradi and Kantzas, 2019). However, what we need to find is that although microfractures are observed by many imaging methods or located by retrieval methods, their characteristics as shale oil and gas transportation channels are still not well figured out (Du et al., 2018a,b). For example, the length, width, geometry and quantitative relationship of microfracture development.

* Corresponding author.
E-mail address: dushuheng@imech.ac.cn (S. Du).

https://doi.org/10.1016/j.egyr.2020.07.004

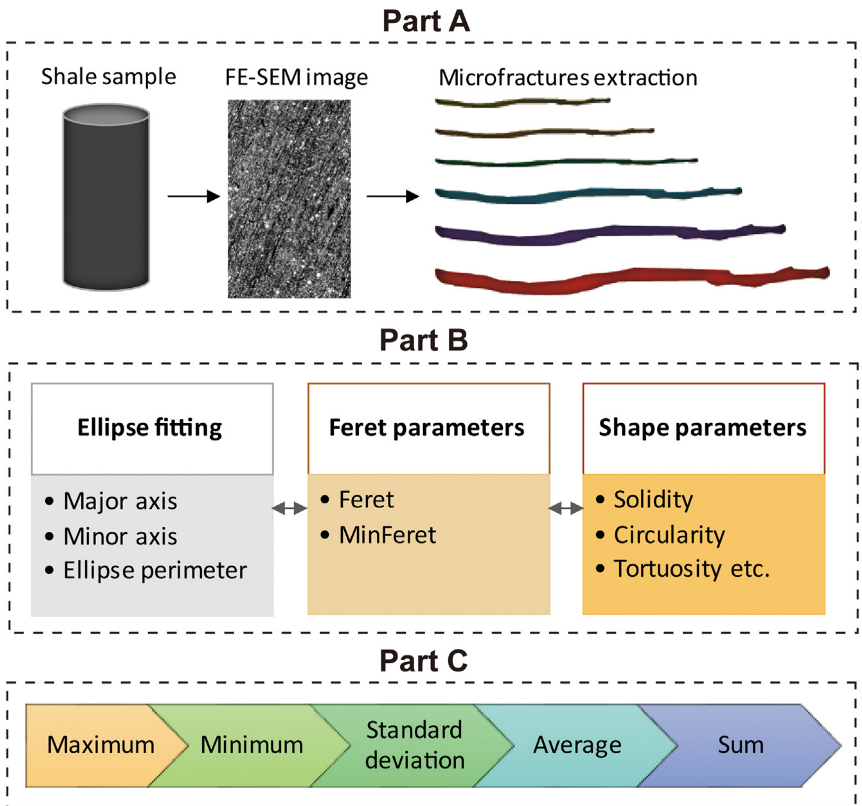

Fig. 1. Technical and theoretical process for the crucial speciality investigation of microfractures in shale (the text color of geometric parameters corresponds to the line color in the schematic map).

As the geometric parameters of microfractures could indicate different geological processes from another aspect, we should continue to dig information from them and try to get a new understanding. Therefore, the key innovation of this paper is to continue to promote the exploration of the geometric properties of microfractures so that more geological significance and engineering significance can be further revealed through microfractures. In the text, we have carried out research on this aspect in close combination with mathematical theory and tools.

2. Technical and theoretical process

Du (2020) have discovered the crucial distinction of the microfractures in tight sandstone reservoir. In this study, we focus on the shale reservoir and try to find some new things.

The samples used in this study are representative hydrocarbon-rich shale reservoirs from a basin in Western China, with high brittleness (the average content of brittle minerals could reach 70%) and developed foliation. The porosity of all samples ranged from 4.8% to 12.6%, with an average of 9.5%. The permeability ranged from 0.1×10^{-3} μm^2 to 0.3×10^{-3} μm^2, with an average of 0.2×10^{-3} μm^2.

The maximum horizontal principal stress direction of the samples in the study area is mainly north-east (the average value is 75 degrees). As the difference of two horizontal stresses at the sampling site is small, which can form a complex fracture network in theory.

The technical and theoretical scheme of this paper could be seen in Fig. 1 and would be divided into three parts.

As to part A, firstly, rock slices are made. Secondly, high-resolution images are got under the field emission scanning electron microscope. Thirdly, all microfractures are identified and extracted. Fracture extraction is mainly based on the method of morphological recognition. Through the image processing program to calculate the ratio of its longitudinal length and transverse length, set the lower limit value of different ratio, compare the extraction effect respectively. Finally, the lowest value corresponding to the best extraction result is selected. Therefore, this is a process of parameter optimization. Finally, we could do the following research on it.

As for the technical details involved in microfracture identification and extraction process, a detailed description can be provided here. All microfractures are extracted from high-resolution backscatter images captured by field emission scanning electron microscope (FE-SEM). The extraction process is handled by combining the authors' own program for the quantitative geometric description on rocks. Meanwhile, we also compare the results with which get by some commercial software include "ImageJ" and "Avizo" to make sure the data precision.

The threshold values of the SEM images have also been determined carefully. First of all, we need to carry out the technology processing of image enhancement and noise removal. Secondly, we use the watershed algorithm to get the initial threshold and initial surface porosity of each sample. Of course, both the initial threshold and the initial face rate need to be optimized furtherly. About the optimization process, we first analyze the correlation degree between the initial surface porosity of each sample's image and the actual measured porosity of each sample. By automatically adjusting the threshold value, we can select the threshold value of each image when the correlation degree reaches the maximum value. That is the threshold we need in the end. Finally, we also check the results of image recognition to ensure that all microfractures are extracted. Through the above methods, we can make sure that the image processing can stand the test.

Identification method of microfractures is a very important technical issue, which can greatly increase the convenience of

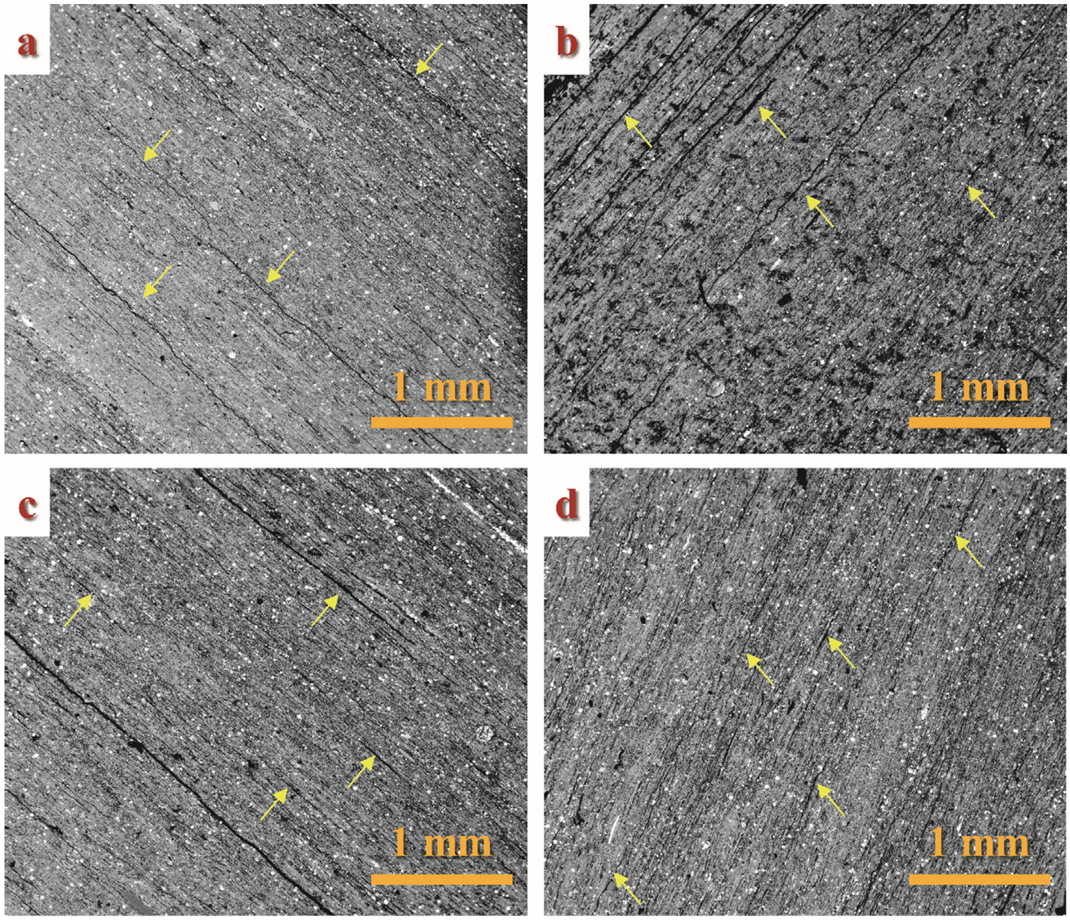

Fig. 2. The microfracture characteristics of shale based on field emission scanning electron microscopy (a, b, c, d are SEM images of typical microfractures of four samples respectively, and the small yellow arrow in the figure indicates the location of microfractures).

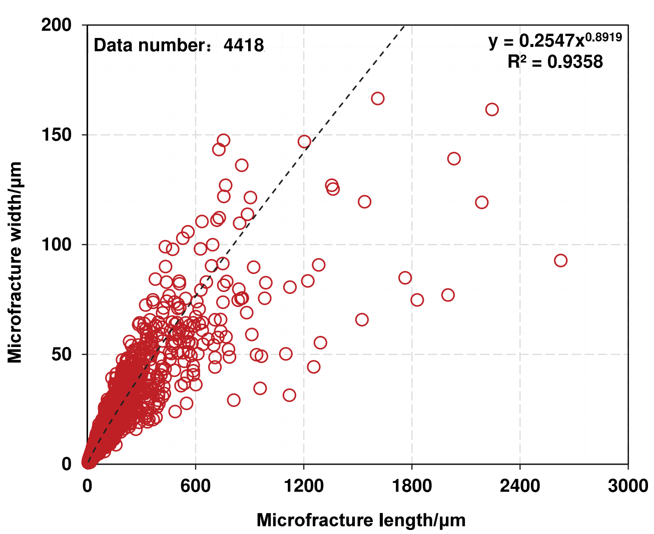

Fig. 3. Relationship between microfractures and microfractures widths in shale reservoir.

research. We calculate the ratio between the longitudinal length and the transverse length of each group of connected pixels (including both real and fake microfractures) extracted from all the sample images. The cumulative frequency distribution curve of this ratio is drawn, and the key segmentation points are identified by analogy with sedimentary geology. When the aspect ratio is higher than the relative value, the individual pixel will be identified as microfractures. This process depends on the properties of the samples. We have examined the microfractures identified by this method, and the recognition accuracy can reach more than 98%.

As to part B, in order to dig out the crucial speciality of microfractures to the greatest extent, three sets of parameters characterizing the size of microfractures from the perspective of computational geometry, combined with Legendre ellipse fitting, Feret diameter calculation and shape factors calculation (Eqs. (1)–(4)).

$$G_1 = 4\pi \frac{S}{P^2} \tag{1}$$

$$G_2 = \frac{L_l}{L_s} \tag{2}$$

$$G_3 = 4\frac{S}{\pi * L_l^2} \tag{3}$$

$$G_4 = \frac{S}{S_c} \tag{4}$$

In Eqs. (1)–(4), "G_1", "G_2", "G_3", and "G_4" indicates the four geometric parameters to describe the microfractures. "S", "P", "L_l", "L_s", "S_c" indicates the area, the perimeter, the major axis of ellipse, the minor axis of ellipse, and the convex area of the microfracture, respectively. As to "G_1" or "G_3", the lower the value, the narrower the microfracture. As to "G_2", the higher the value, the narrower and longer the microfracture. As to "G_4", the lower the value, the more concave the microfracture. Measurements of all the parameters could be carried out by the imaging processing program effectively.

The maximum and minimum of Feret diameter of microfractures, indicate the length and width of microfractures, respectively. Similarly, the major and minor axis of ellipse could also indicate the length and width in another aspect. In addition, as to microfractures, the average degrees of concave and convex (solidity) in could be used as indicative parameters of reservoir compaction. The lower the solidity of microfracture, the higher the degree of compaction (Du, 2020).

Meanwhile, the greater the tortuosity, the more uneven the boundary of microfractures. The smaller the circularity, the higher the ellipticity and the more uneven the boundary of microfractures, too. It should be pointed out that above four parameters are all described from the perspective of geometry. In practical application, they should be combined to indicate deeper geological or engineering significance. Of course, the rationalities of above those parameters still need to be tested and improved in practice and more parameters with clear physical meaning will gradually appear.

In part C, we calculated and counted each attribute's maximum, minimum, standard deviation (one value per sample), average value and sum of 4410 microfractures in 42 samples, hoping to make a final summary of the development of microfractures in shale.

3. Results

Field emission scanning electron microscopy (FE-SEM) is one of the most advanced means to observe microfractures. In order to show the development characteristics of microfractures in shale reservoirs in the study area intuitively, we used FE-SEM to get and select typical images of microfractures in shale under high-resolution mode (Fig. 2). These pictures show the fact that there are a lot of microfractures develop in shale. Their characteristics are worthy to be further explored.

3.1. Feret (length) and MinFeret (width)

In Fig. 3, it can be seen that the length and width of microfractures are positively correlated as a whole, when the microfracture length is less than about 300 μm (corresponding to the width of microfracture is less than about 65 μm), they show a good linear positive correlation, but when the length of microfracture continues to increase, the width of microfracture gradually deviates from the linear relationship and gradually diverges.

It is proved that there is a critical threshold value for the length (or width) of microfractures. When the threshold value is not reached, the rock structure does not change substantially, and the fracture process tends to be stable. When the threshold value of length (or width) is reached, the microfractures formed in the rock have caused some essential changes in the rock structure, and then the fracture process tends to be "Unsteady".

Meanwhile, standard deviation of the length and width values of all microfractures and their cross-plot diagrams are made (Fig. 4). It shows the greater the fluctuation degree of microfracture length value, the greater the fluctuation degree of width value which is the good responses to the instability of the formation of microfractures referred above.

3.2. Major and minor axis in ellipse of microfractures

Similarly, in Fig. 5, it can be seen that the major and minor axis values of microfractures are positively correlated as a whole, when the microfracture length is less than about 250 μm (corresponding to the width of microfracture is less than about 30 μm),

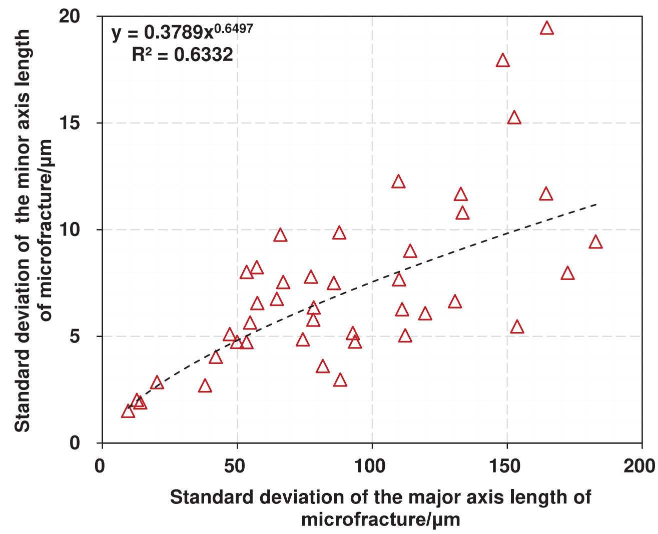

Fig. 4. Standard deviation relationship between microfractures lengths and microfractures widths in shale reservoir.

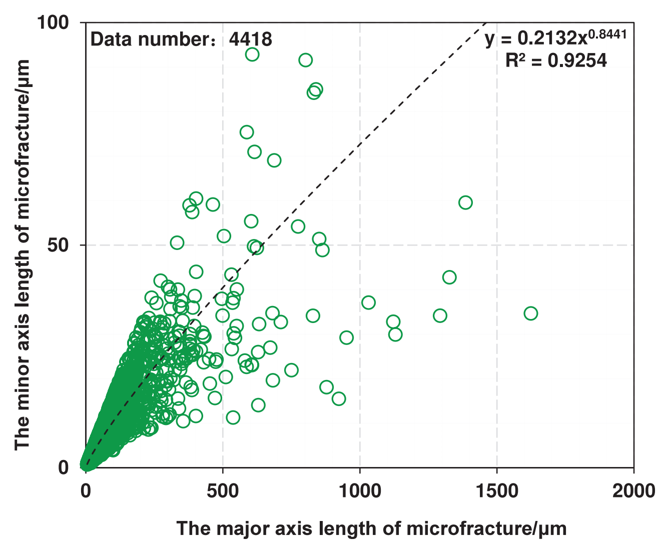

Fig. 5. Relationship between standard deviation of the major and minor axis value of microfractures in shale reservoir.

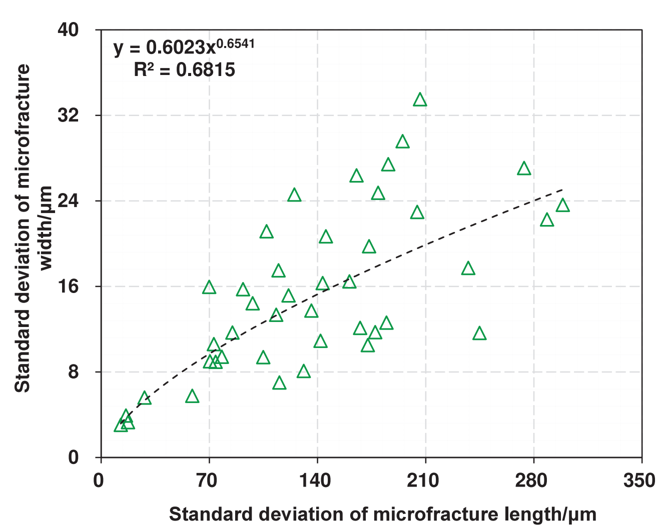

Fig. 6. Standard deviation relationship between microfracture lengths and widths of microfracture in shale reservoir.

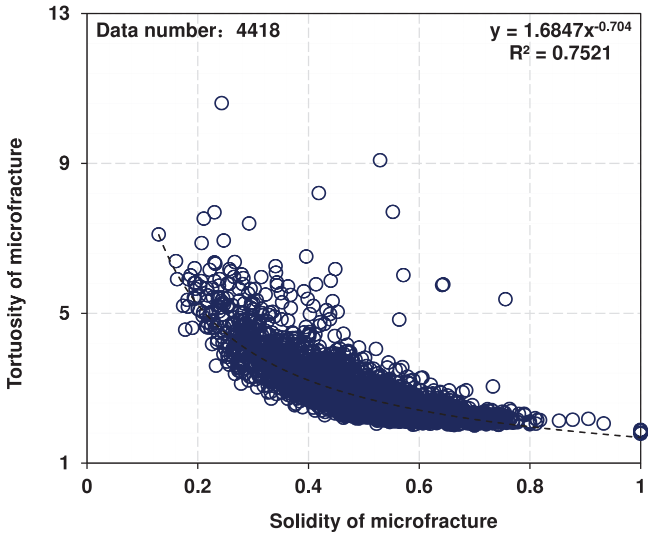

Fig. 7. Relationship between microfracture solidity values and the new tortuosity values in shale reservoir.

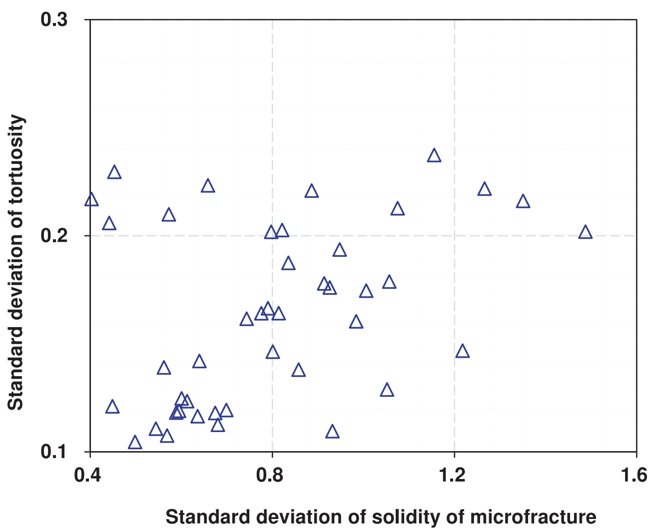

Fig. 8. Standard deviation relationship between microfracture solidity values and the new tortuosity values in shale reservoir.

they show a good linear positive correlation, but when the major axis length of microfracture continues to increase, the minor axis of microfracture gradually deviates from the linear relationship and gradually diverges.

Meanwhile, standard deviation Relationship between the two type of values of all microfractures shows the greater the fluctuation degree of microfractures' major axis lengths, the greater the fluctuation degree of minor axis lengths which is also the good responses to the instability of the formation of microfractures referred above (Fig. 6).

3.3. Solidity and tortuosity in microfractures

Microfracture, as a key type of seepage channel, the tortuosity of it refers to the ratio of the actual length of the fluid passing through it to the apparent length (macro distance) of the fluid passing through it (Du, 2020).

In order to explore the relationship between the degree of compaction and the degree of dissolution of microfractures, the

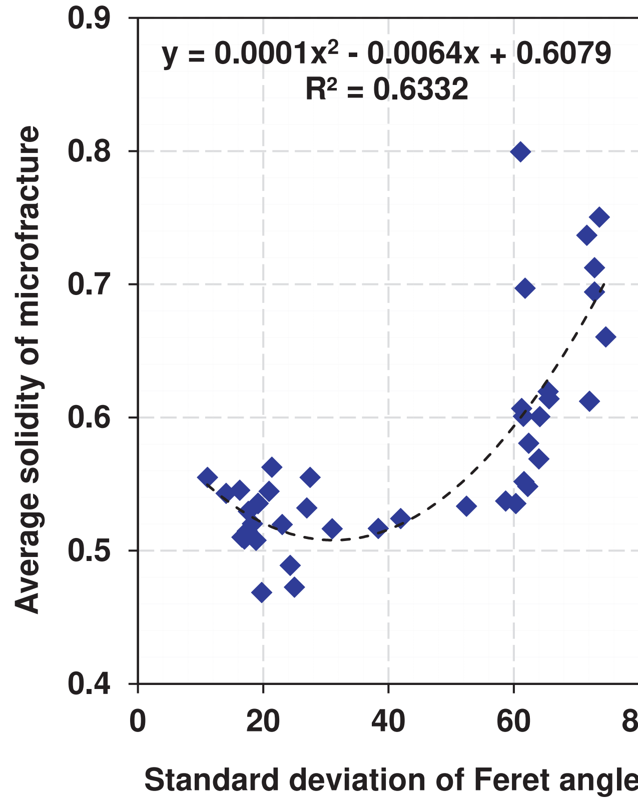

Fig. 9. Relationship between standard deviation of Feret angle and average tortuosity in shale reservoir.

correlation regression between the solidity and tortuosity is made (Fig. 7).

With the power exponential increase of compression degree (i.e. the solidity value of microfractures gradually decreases), the tortuosity value of microfractures gradually increases, and the rate of increase gradually increases (Fig. 7).

However, the cross-plot results of standard deviation show that the relationship between compaction heterogeneity and pressure solution heterogeneity is not obvious. This means that compaction or other tectonic stress can promote the formation of shale microfractures and promote the occurrence of pressure solution. However, actually, there are many control factors leading to pressure solution, not only compaction, but also the influence of acid fluid properties, thermodynamics and other factors, which deserve our further attention (Fig. 8).

4. Geological significance of microfracture description

In order to figure out the formation mechanism of microfracture from the geometric aspect, cross-plots related to each attribute's maximum, minimum, standard deviation (one value per sample), average value and sum of 4410 microfractures in 42 samples are drawn.

4.1. Microfracture orientation degree and other attributes

By plotting the cross-plot between the standard deviation of microfracture extension angle (the reciprocal of orientation degree) and the average solidity, it is easy to find that there is a quadratic relationship between them. The convexity of microfractures (solidity) decreases first and then increases with the improvement of orientation (the standard deviation of angle decreases gradually). This indicates that before a certain key

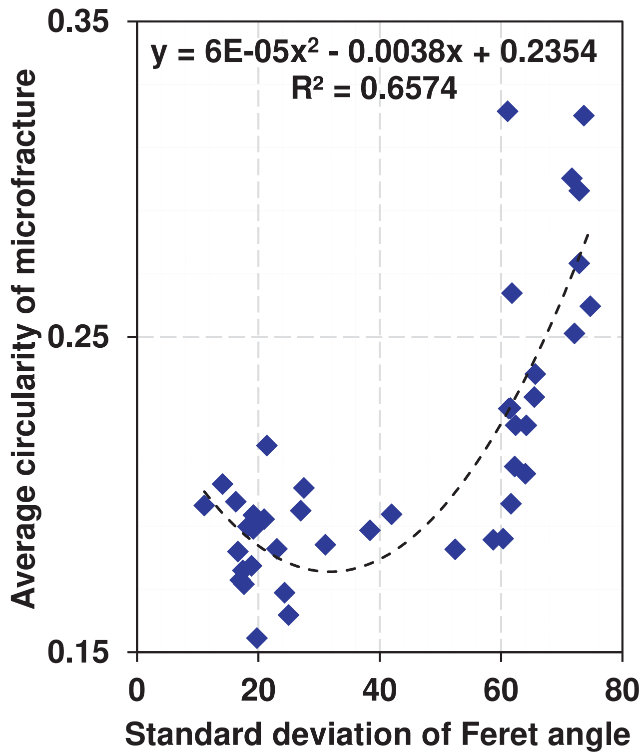

Fig. 10. Relationship between standard deviation of Feret angle and average circularity in shale reservoir.

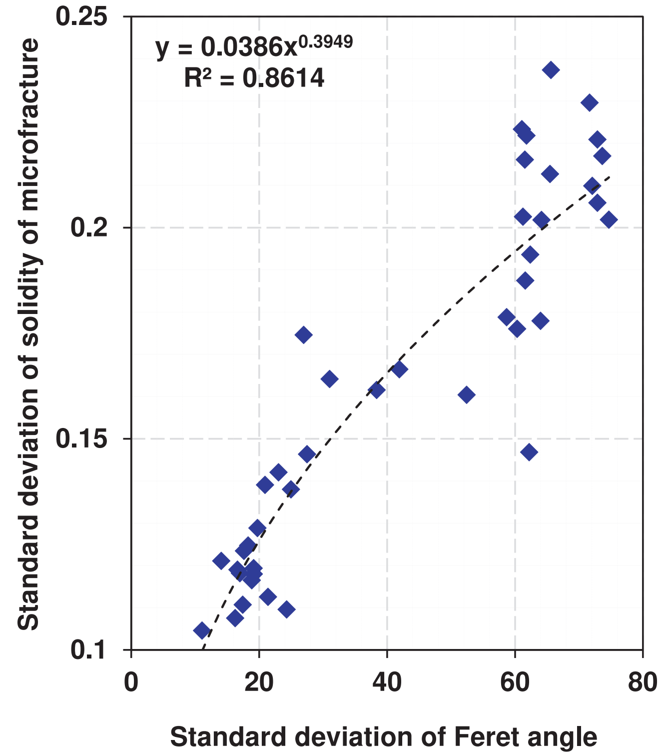

Fig. 12. Relationship between standard deviation of Feret angle and standard deviation of solidity in shale reservoir.

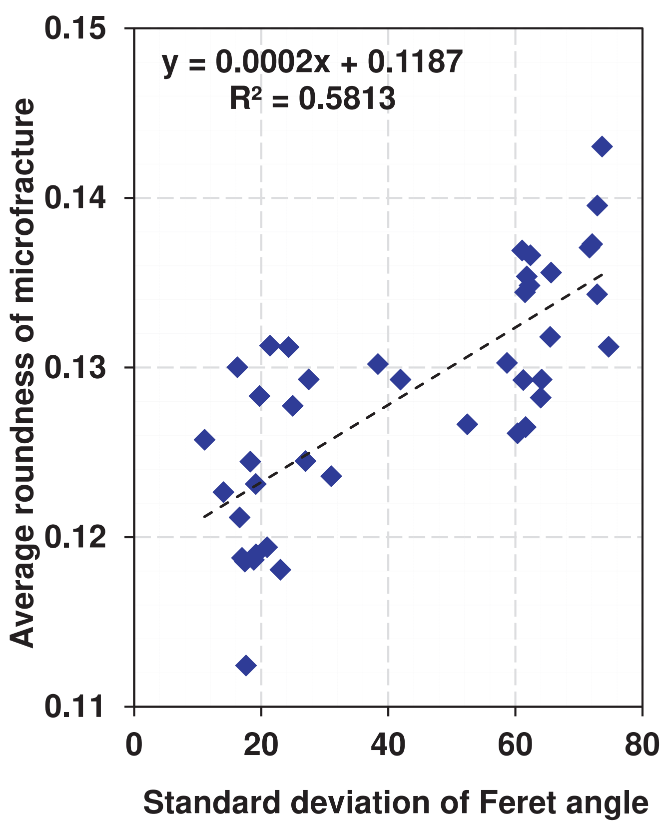

Fig. 11. Relationship between standard deviation of Feret angle and average roundness in shale reservoir.

point, the poor orientation degree of microfractures often coexists with the higher convexity of microfractures, which is positively correlated. When this key point is crossed, the two begin to show a negative correlation. This may be due to the fact that the microfractures will open, close, extend or even interlace more frequently when the rock is under complex stress conditions (Fig. 9).

Similarly, by plotting the cross-plot between the orientation degree and the average circularity, it is easy to find that before a certain key point, the poor orientation degree of microfractures often coexists with the higher circularity of microfractures, which is positively correlated. When this key point is crossed, the two begin to show a negative correlation. This could also prove the complex mechanics behavior of microfractures rock under complex stress conditions (Fig. 10).

By plotting the cross-plot between the Feret angle and the average roundness, it is easy to find that there is a linear relationship between them. This means that the better the orientation degree, the lower the roundness of the microfractures (Fig. 11). At the same time, it is proved that the change of the roundness and directionality of microfractures is consistent in general.

Fig. 12 shows that as the orientation of microfracture in each sample becomes better (the extension angles of microfracture become more homogeneous), the heterogeneity of the solidity of microfracture becomes more obvious. This shows that with the increasing of the heterogeneity of compaction, the orientation degree will be worse and worse. This proves that good orientation degree is generally closely related to the homogeneity of compaction.

Similarly, Fig. 13 shows that as the orientation of microfracture in each sample becomes better (the extension angles of microfracture become more homogeneous), the heterogeneity of the circularity of microfracture becomes more obvious, which is certainly realistic.

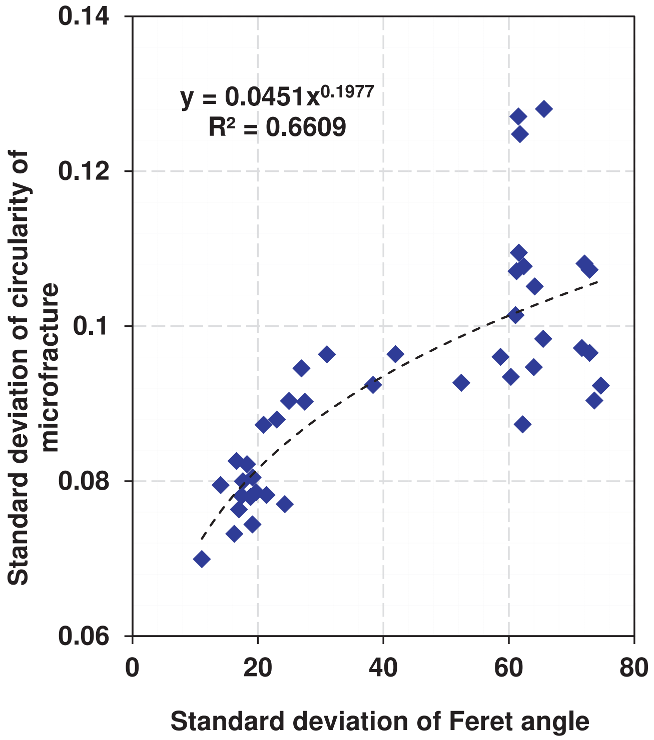

Fig. 13. Relationship between standard deviation of Feret angle and standard deviation of circularity in shale reservoir.

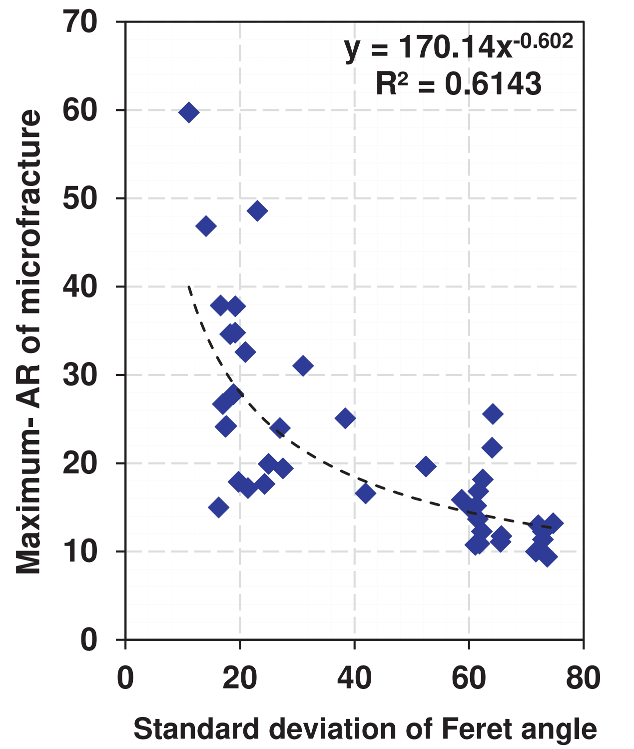

Fig. 14. Relationship between standard deviation of Feret angle and average aspect ratio (AR) in shale reservoir.

Relationship between standard deviation of Feret angle and maximum of aspect ratio (AR) shows that the better the orientation degree, the larger the maximum of aspect ratio (Fig. 14). At the same time, from the initial stage, the decrease of orientation degree will be accompanied by the rapid decrease of the maximum aspect ratio. Then, as the orientation degree becomes worse, the absolute value of the maximum aspect ratio is still decreasing, but its decreasing rate (curve slope) is gradually decreasing. This is an interesting phenomenon (Fig. 14).

Sum of the fitted ellipse perimeter could represent the actual streamline length approximately. Relationship between standard deviation of Feret angle and sum of the fitted ellipse perimeter may convey some other crucial meanings. It shows that the better the orientation degree, the larger the sum of the fitted ellipse perimeter (Fig. 15). In other words, the longer the boundary of microfracture is, the better the orientation degree of microfracture is.

4.2. Maximum and minimum of microfracture attributes

For all the 42 samples, there are nearly 105 microfractures in each sample. Among these microfractures of a single sample, there must be a microfracture with the maximum perimeter value and a microfracture with the maximum length value. Sometimes, the same fracture has both the maximum perimeter value and the maximum length value. It is known from Fig. 16 that the minimum circularity of microfracture decreases with the increase of the maximum length and perimeter of microfracture. In fact, for the same sample, the microfracture with the largest perimeter and length value may also be the microfracture with the smallest circularity. This is not contradictory (Fig. 16).

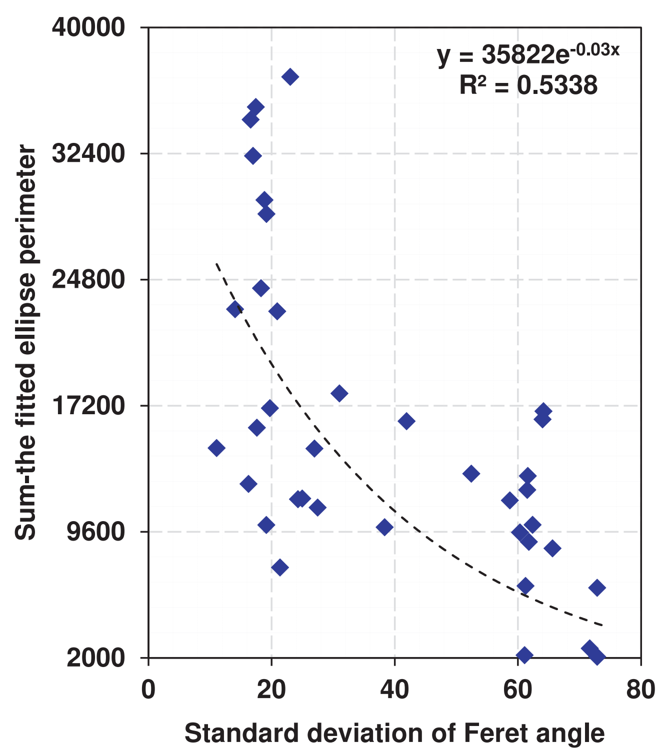

Fig. 15. Relationship between standard deviation of Feret angle and sum of ellipse perimeter in shale reservoir.

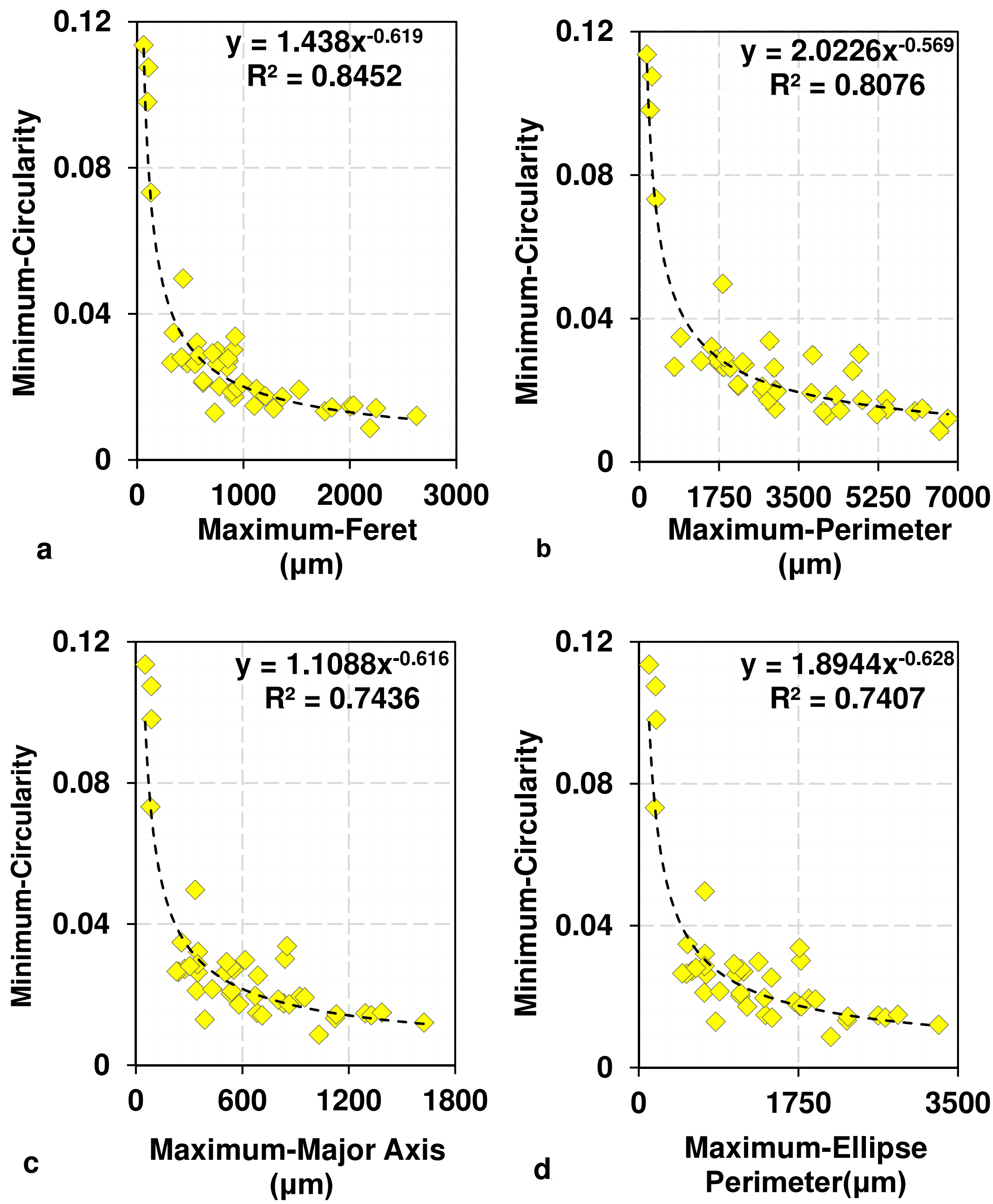

Fig. 16. Relationship between maximum and minimum of microfracture attributes.

Table 1
Statistics of maximum, minimum, standard deviation, average value and sum of 4410 microfractures size.

Value\Properties	Perimeter (μm)	Ellipse perimeter (μm)	Major (μm)	Minor (μm)	Feret (μm)	MinFeret (μm)
Maximum	6778.00	3287.56	1624.00	92.82	2626.00	166.50
Minimum	10.31	10.53	4.87	0.70	5.15	0.73
Average	218.61	133.22	62.89	6.53	83.74	11.90
Homogeneity coefficient	0.03	0.04	0.04	0.07	0.03	0.07

4.3. Statistics of microfracture properties

As can be seen in Tables 1 and 2, each attribute's maximum, minimum, standard deviation (one value per sample), average value and sum of 4410 microfractures in 42 samples are calculated and counted.

As to microfractures size (Table 1), we could see that although the absolute value of the maximum, minimum and average of the six size attributes varied, the homogeneity coefficients of these parameters are nearly the same. It is well proved that the heterogeneities of multiple size parameters of microfractures are basically the same. However, we should also be aware that for a

Table 2
Statistics of maximum, minimum, standard deviation, average value and sum of 4410 microfractures geometry.

Value\Properties	AR	Tortuosity	Circularity	Solidity
Maximum	59.73	10.61	0.43	1.00
Minimum	6.24	1.78	0.01	0.13
Average	8.61	2.73	0.20	0.55
Homogeneity coefficient	0.14	0.26	0.46	0.55

single size parameter, the value of its homogeneity coefficient is very low.

Similarly, as to microfractures geometry (Table 2), the absolute values of the maximum, minimum and average of the six geometry attributes are varied, but the homogeneity coefficients of these parameters are also varied. It proved that geological process is complex, leading to the main control factors of each geometric parameter are different, so the heterogeneity of each geometric parameter of microfractures is different, too.

In a word, the geometric properties of microfractures has great potential to reveal the heterogeneity of microfractures development. Special attention should be paid in practical application.

5. Conclusions

As to microfractures in shale, Feret (length) and MinFeret (width), major and minor axis of ellipse, solidity and tortuosity could be the key factors reflecting the formation mechanism. As to the above parameters, it is proved that there are critical threshold values for the microfractures growth. When the threshold value is not reached, the rock structure does not change substantially, and the geological process of fracturing tends to be stable. When the threshold value of length (or width) is reached, the microfractures formed in the rock have caused some essential changes in the rock structure, and then the fracture process tends to be "unsteady". This could also be applicable to other unconventional reservoirs which need to be paid more attention to.

However, we also need to realize that, compared with a single size parameter, for a single geometric parameter, the value of its homogeneity coefficient is generally one order of magnitude larger than that of a single size parameter. In other words, the size and geometric parameters of microfractures would represent the heterogeneity at different aspects. This could also gives us a enlightenment, that is, when describing the heterogeneity characteristics of microfractures, we should clearly describe them from two aspects of size and geometry, so as to ensure the integrity of the conclusion.

We hope that through this research, scholars can clarify the critical specificity of microfractures in shale as the independent transportation channels. Then the other researchers can follow this path and get more and better scientific understanding with practical significance.

Declaration of competing interest

The authors declare that they have no known competing financial interests or personal relationships that could have appeared to influence the work reported in this paper.

Acknowledgments

This work was jointly supported by Open Fund of State Key Laboratory of Shale Oil and Gas Enrichment Mechanisms and Effective Development (Grant No. 10010099-19-ZC0607-0034), National Natural Science Foundation of China (NSFC, Grant No. 41902132, 11872363, 51861145314), PetroChina Innovation Foundation (Grant No. 2019D-5007-0214), Chinese Academy of Sciences (CAS) through the CAS Key Research Program of Frontier Sciences (Grant No. QYZDJ-SSW-JSC019) and the CAS Strategic Priority Research Program (Grant No. XDB22040401). Thanks very much for the recognition of this research by the academic editor and the reviewers of the journal.

References

Abouelresh, M.O., 2017. An integrated characterization of the porosity in Qusaiba Shale, Saudi Arabia. J. Petrol. Sci. Eng. 149, 75–87.
Chauve, T., Scholtès, L., Donzé, F.V., Mondol, N.H., Renard, F., 2019. Microfracture propagation in layered shale rocks during primary migration. In: Geophysical Research Abstracts, vol. 21.
Clarke, C.E., Bugden, D., Hart, P.S., Stedman, R.C., Jacquet, J.B., Evensen, D.T., Boudet, H.S., 2016. How geographic distance and political ideology interact to influence public perception of unconventional oil/natural gas development. Energy Policy 97, 301–309.
Du, S., 2019. Prediction of permeability and its anisotropy of tight oil reservoir via precise pore-throat tortuosity characterization and umbrella deconstruction method. J. Petrol. Sci. Eng. 178, 1018–1028.
Du, S., 2020. Characteristics and the formation mechanism of heterogeneous microfracture in the upper Triassic Yanchang formation tight oil sandstone of the Ordos Basin, China. J. Petrol. Sci. Eng. 191, 107176.
Du, S., Pang, S., Shi, Y., 2018a. A new and more precise experiment method for characterizing the mineralogical heterogeneity of unconventional hydrocarbon reservoirs. Fuel 232, 666–671.
Du, S., Pang, S., Shi, Y., 2018b. Quantitative characterization on the microscopic pore heterogeneity of tight oil sandstone reservoir by considering both the resolution and representativeness. J. Petrol. Sci. Eng. 169, 388–392.
Du, S., Shi, Y., Zheng, X., Chai, G., 2020. Using umbrella deconstruction & energy dispersive spectrometer (UD-EDS) technique to quantify the anisotropic elements distribution of Chang 7 shale and its significance. Energy 191, 116443.
Du, S., Xu, F., Taskyn, A., Zhou, B., Kou, G., Shi, Y., 2019a. Anisotropy characteristics of element composition in Upper Triassic Chang 8 shale in Jiyuan district of Ordos Basin, China: Microscopic evidence for the existence of predominant fracture zone. Fuel 253, 685–690.
Du, S., Zhao, Y., Jin, J., Kou, G., Shi, Y., Huang, X., 2019b. Significance of the secondary pores in perthite for oil storage and flow in tight sandstone reservoir. Mar. Pet. Geol. 110, 178–188.
Elwegaa, K., Emadi, H., 2019. Improving oil recovery from shale oil reservoirs using cyclic cold nitrogen injection–An experimental study. Fuel 254, 115716.
Gupta, A., Xu, M., Dehghanpour, H., Bearinger, D., 2017. Experimental investigation for microscale stimulation of shales by water imbibition during the shut-in periods. In: SPE Unconventional Resources Conference. Society of Petroleum Engineers.
Huang, L., Liu, J., Zhang, F., Dontsov, E., Damjanac, B., 2019. Exploring the influence of rock inherent heterogeneity and grain size on hydraulic fracturing using discrete element modeling. Int. J. Solids Struct. 176, 207–220.
Khan, N.A., Engle, M., Dungan, B., Holguin, F.O., Xu, P., Carroll, K.C., 2016. Volatile-organic molecular characterization of shale-oil produced water from the Permian Basin. Chemosphere 148, 126–136.
Kilian, L., 2016. The impact of the shale oil revolution on US oil and gasoline prices. Rev. Environ. Econ. Policy 10 (2), 185–205.
Kondash, A.J., Albright, E., Vengosh, A., 2017. Quantity of flowback and produced waters from unconventional oil and gas exploration. Sci. Total Environ. 574, 314–321.
Lesniak, G., Cicha-Szot, R., Such, P., (2017). The role of microfractures in shale rocks. In EGU General Assembly Conference Abstracts, vol. 19, 12497.
Madasu, S., Nguyen, P.D., 2017. Computational and experimental study of microfracture conductivity in the Eagle Ford shale using microproppant pillars. In: SPE Reservoir Characterisation and Simulation Conference and Exhibition. Society of Petroleum Engineers.
Middleton, R.S., Gupta, R., Hyman, J.D., Viswanathan, H.S., 2017. The shale gas revolution: Barriers, sustainability, and emerging opportunities. Appl. Energy 199, 88–95.
Mohammadmoradi, P., Kantzas, A., 2019. Modelling shale spontaneous water intake using semi-analytical and numerical approaches. Can. J. Chem. Eng. 97, 1627–1642.
Ougier-Simonin, A., Renard, F., Boehm, C., Vidal-Gilbert, S., 2016. Microfracturing and microporosity in shales. Earth-Sci. Rev. 162, 198–226.
Panahi, H., Kobchenko, M., Meakin, P., Dysthe, D.K., Renard, F., 2019. Fluid expulsion and microfracturing during the pyrolysis of an organic rich shale. Fuel 235, 1–16.
Pluymakers, A., Kobchenko, M., Renard, F., 2017. How microfracture roughness can be used to distinguish between exhumed cracks and in-situ flow paths in shales. J. Struct. Geol. 94, 87–97.

Teixeira, M.G., Donzé, F., Renard, F., Panahi, H., Papachristos, E., Scholtès, L., 2017. Microfracturing during primary migration in shales. Tectonophysics 694, 268–279.

Ukar, E., Lopez, R.G., Laubach, S.E., Gale, J.F., Manceda, R., Marrett, R., 2017. Microfractures in bed-parallel veins (beef) as predictors of vertical macrofractures in shale: Vaca Muerta Formation, Agrio Fold-and-Thrust Belt, Argentina. J. South Am. Earth Sci. 79, 152–169.

Wachtmeister, H., Lund, L., Aleklett, K., Höök, M., 2017. Production decline curves of tight oil wells in eagle ford shale. Natural Resour. Res. 26 (3), 365–377.

Zhang, F., Damjanac, B., Maxwell, S., 2019. Investigating hydraulic fracturing complexity in naturally fractured rock masses using fully coupled multiscale numerical modeling. Rock Mech. Rock Eng. 52 (12), 5137–5160.

Zhao, Y.P., 2016. Modern Continuum Mechanics. Science Press, China, Beijing.

Zhao, Y.P., 2018. Lectures on Mechanics. Science Press, China, Beijing.

Zhu, H., Tang, X., Liu, Q., Li, K., Xiao, J., Jiang, S., McLennan, J.D., 2018. 4d multi-physical stress modelling during shale gas production: A case study of Sichuan Basin shale gas reservoir, China. J. Petrol. Sci. Eng. 167, 929–943.